

Technoeconomic Optimization of a Recuperator Considering Pressure Drops and Operating Costs

Bir Reküperatörün Basınç Düşüşleri ve İşletme Maliyetleri Göz önünde bulundurularak Teknoekonomik Optimizasyonu

Erhan KAYABASI¹ 

¹ Karabuk University, Engineering Faculty, Mechanical Engineering Department, Karabuk, Turkey

Abstract

In this study, heat transfer and cost optimization of a gas-to-gas heat exchanger (recuperator) operating in the targeted temperature range has been made. Firstly, the thermophysical properties of the waste heat source and the volumetric flow rates of the flows were obtained, and the maximum heat that could be recovered was obtained. Afterward, a parametric study was carried out to size the recuperator. The parameters affecting the cost, such as hot flow and cold flow outlet temperatures, were determined by the overall heat transfer coefficient, effectiveness, and pressure drop. Finally, the thermal parameters obtained from the parametric study are used in the technoeconomic analysis. The recuperator geometry with the maximum saving coefficient was determined considering investment and operating costs. As a result, the 108th simulation resulted in maximum savings with 653 252 \$/year using 321.19 m² heat transfer surface area. Efficiency, overall heat transfer coefficient and pressure drops for cold and hot flow were obtained as 0.65, 107.3 W/m²K 0.024 and 0.022 bar, respectively.

Keywords: waste heat recovery, cost optimization, dimension optimization, technoeconomy, recuperator

Öz

Bu çalışmada, hedeflenen sıcaklık aralığında çalışan bir gazdan gazı ısı değiştiricinin (reküperatör) ısı transferi ve maliyet optimizasyonu yapılmıştır. Öncelikle atık ısı kaynağının termofiziksel özellikleri ve akışların hacimsel debileri elde edilerek geri kazanılabilecek maksimum ısı elde edilmiştir. Daha sonra reküperatörü boyutlandırmak için parametrik bir çalışma yapılmıştır. Sıcak akış ve soğuk akış çıkış sıcaklıkları gibi maliyeti etkileyen parametreler, toplam ısı transfer katsayısı, etkinlik ve basınç düşüşü dikkate alınarak belirlendi. Son olarak, parametrik çalışmadan elde edilen termal parametreler teknoekonomik analizde kullanılmıştır. En yüksek tasarruf katsayısına sahip reküperatör geometrisi, yatırım ve işletme maliyetleri dikkate alınarak belirlenmiştir. Sonuç olarak, 108. Simülasyonda elde edilen geometrideki reküperatörün 321.19 m² ısı transfer yüzey alanı ile yılda 653 252 \$ ile maksimum tasarruf sağlayabileceği tespit edilmiştir. Etkenlik, toplam ısı transfer katsayısı ve soğuk ve sıcak akış için basınç düşüşleri sırasıyla 0.65, 107.3 W/m²K 0.024 ve 0.022 bar olarak elde edilmiştir.

Anahtar Kelimeler: Atık ısı geri kazanımı, aliyet optimizasyonu, boyut optimizasyonu, teknoekonomi, reküperatör

I. INTRODUCTION

The recovery of waste heat from industrial operations is crucial for reducing production costs and emissions in addition to the effective use of energy in industrial processes. In particular, the flue gases between 900 °C - 1600 °C arising from the high-temperature melting processes between 1650 °C-1750 °C in iron and steel production are considered as a secondary energy source [1-3]. Heat exchangers, useful static devices operating without consuming energy, are frequently used in industrial processes to utilize wasted thermal energy [4,5]. Gas-to-gas heat exchangers (recuperators) located between the furnace and stack consists of tube bundles used for heat recovery from flue gas in high temperature to combustion air used in the burning process [6,7]. Since the fluids in recuperators are gas, the total heat transfer coefficient is lower than the liquid heat exchangers, so a relatively higher heat transfer area is required. The increased surface area increases the volume that needs to be allocated inside the factory to install heat exchangers and the investment costs. Therefore, the size optimization of the recuperator should be done precisely to achieve heat recovery with the lowest heat transfer surface area and the lowest cost [8,9]. Many methods and tools have been used for this purpose. For example, Dehaj and Hajabdollahi [10] studied thermoeconomic optimization on fin and tube heat to achieve an optimum construction. They used a multi-objective genetic algorithm to optimize the heat exchanger structure, employing effectiveness and total annual cost in the objective function. They reached a maximum 6.65% increase in effectiveness value. Söylemez [11] studied the cost optimization of heat pipe heat exchangers using ϵ -NTU and P_1 - P_2 methods. He achieved 50 \$/(W/K) savings, optimum effectiveness of 0.8. Manjunath et al. [12] calculated entropy generation and made a

thermoeconomic analysis of printed circuit heat exchangers by different construction materials. As a result, although hastelloy-N showing a higher second law efficiency than stainless steel, it is not cost-effective. Sahin et al. [13] studied numerically using cost and performance analysis on counterflow single-pass heat exchangers. They used heat transfer rate cost as an objective function considering total exergy loss and investment cost. They achieved the maximum objective function value while the heat capacity ratio is 1, NTU is 12, and effectiveness is 0.93. Maghsoudi et al. [14] studied a thermoeconomic investigation to improve the performance of plate-finned recuperators by employing the NSGA-II algorithm and DEA model. Consequently, they achieved 0.81 effectiveness and 0.716 kPa pressure drop with 326 688 \$ cost. Zhenyu and Huier [15] studied the optimization of design parameters using a multi-objective optimization model considering heat transfer performance, heat exchanger weight, and pressure loss. As a result, they discovered that corrugated foil geometries should be avoided for better performance. Hu et al. [16] studied the 1-D dynamic model of an S-CO₂ cycle recuperator considering the physical properties of the flows, temperatures, and pressures using MATLAB. They have discovered the physical properties variations of the flows in recuperator depending on time domain in detail. In order to achieve high heat flux, Chen and Liu [14] researched the design of the recuperator in Hampson cryocoolers based on the low pressure drop theory rather than the low temperature difference [17]. As a result of the study equivalent average temperature was decreased by 30%. As summarized in previous studies, most of the studies are focused on the dimensions, temperature distributions and heat flux etc., with limited variations and without considering the investment and operating costs with the aid of artificial intelligence algorithms. However, there is wide gap in the researches on comprehensive studies performed on numerous options using well developed commercial software and considering the both the investment and operating costs in order to determine the optimum geometric dimensions, effectiveness, pressure drop and heat transfer coefficient that providing maximum saving.

This study focuses on the sizing of a gas-to-gas heat exchanger was studied parametrically using the Simcenter Flomaster software. The optimum heat exchanger dimensions with the lowest saving coefficient were precisely determined. Firstly, the flow rates and temperatures of the recuperator flue gas and fresh air to be heated were selected. Afterward, the recuperator was modeled 1-D parametrically in Simcenter Flomaster software. Simulations were made by giving the initial dimensions. In addition,

dimensionless savings coefficients were obtained for each simulation result using the factory thermal energy production costs and unit cost of heat transfer area. Finally, optimal recuperator dimensions have been determined considering the furnace operating conditions. Thus, the thermal, dimensional and economic optimization of a recuperator has been realized in a versatile way.

II. MATERIALS AND METHODS

This study consists of three main steps: determining the operating conditions under operating conditions, simulating the recuperator dimensions parametrically and economic optimization.

1.1. Operating conditions

In the facility where the recuperator will be operated, the combustion air used in the reheating furnace is heated with the flue gas. The flue gas temperature and flow rate were measured with Testo 350 flue gas analyzer to obtain the thermophysical properties, flue gas mass flow rate. As a result of the flue gas analysis, flue gas contains 6.2% O₂, 7.8% CO₂, 15.9% H₂O and 70.1% N₂. The flue gas and atmospheric air temperature values are 650 °C and 20 °C, respectively.

The flue gas content and volumetric ratios were identified in the Simcenter Flomaster software. The heat transfer coefficient, specific heat, dynamic viscosity, and kinematic viscosity values of the flue gas were calculated depending on the temperature variation. Thus, the simulations were carried out according to changing temperatures to flue gas and combustion air thermophysical properties.

1.2. Recuperator dimensions

Flue gas rejected from the furnace with a mass flow rate of 12.5 kg/s and a temperature of 650°C enters the recuperator as mixed crossflow through the banks of tubes. Unmixed internal flow of combustion air with a mass flow rate of 8.3 kg/s and a temperature of 20 °C enters the recuperator. To avoid H₂O concentration in the flue gas condensing, the outlet temperature of flue gas is anticipated to be greater than 120°C. The flows' outlet pressures were set at 1 bar. The general layout of the entire process that the recuperator installment proposed is given in Figure 1. Cold flow has two passages, and hot flow has one passage across the recuperator, as shown in Figure 2a. The recuperator pipe arrangement has been chosen as an aligned arrangement.

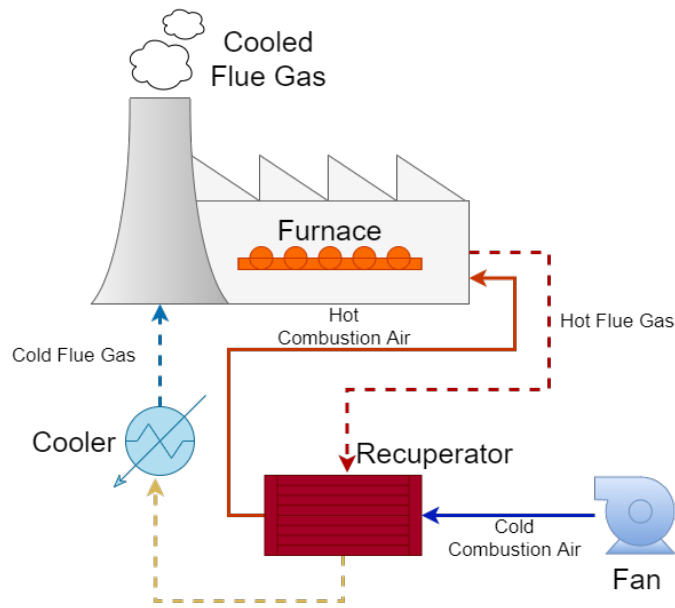


Figure 1. Flow chart of the total system for the proposed recuperator.

One dimensional model of the flow paths in the recuperator was modeled using Simcenter Flomaster software, as given in Figure 2b. Simcenter Flomaster is helpful software that can model one-dimensional thermo-fluid systems. It permits the creation of virtual networks and models the behavior of thermo-fluid systems under various conditions, including steady-state and transient. It is also possible to model existing "real world" systems to predict behavior under varying conditions or design new techniques, to develop a virtual version before committing to building it. Simcenter Flomaster contains the calculations, curves,

and surfaces required to predict the behavior of a range of fluid systems. These calculations are held in Component Analytical Models (CAMs), which form the basis of "components" building blocks of virtual fluid systems. It simulates fluid systems parametrically as networks that comprise connected components, each with its own set of results, such as volumetric flow rate, total heat flow, and pressure. Additionally, different types of simulation (depending upon your license type), such as incompressible, compressible, heat transfer and two phases, are also possible to simulate accurately [18].

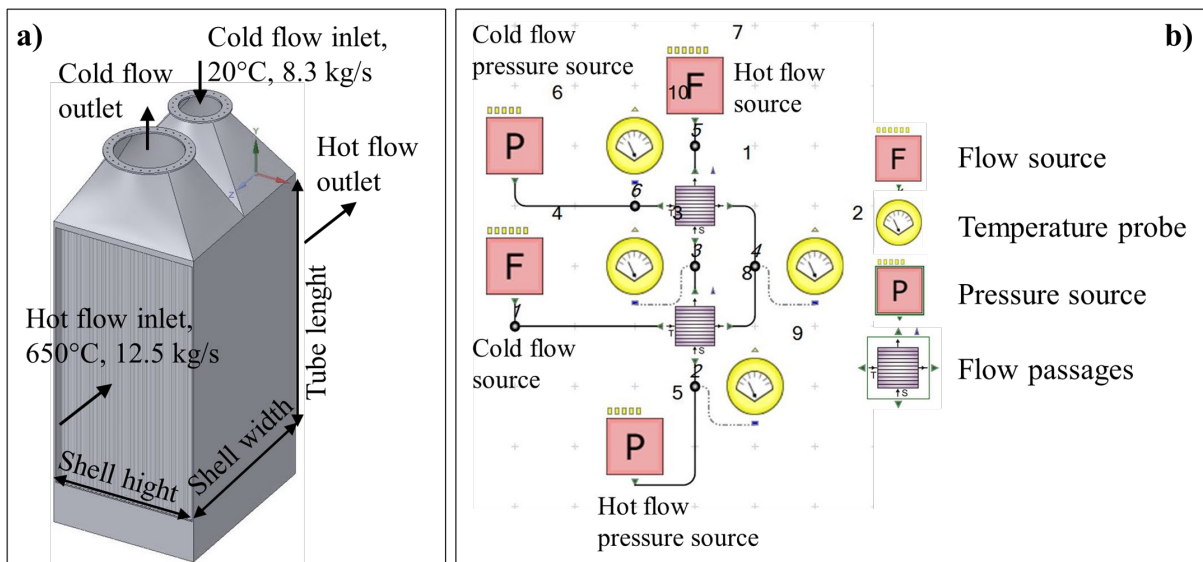


Figure 2. The general arrangement of the recuperator: a) 3D model, b) cell model.

Flow sources permit the definition of mass flow rates and inlet temperatures of the flows. Pressure sources are used for the pressure conditions through the flow. Temperature probes are imaginary measurement

devices to read the temperature values of the nodes between the passages and the sources. In this study, two flow and pressure sources for hot and cold flow, four

temperature probes, two for outlets and two for the nodes between the passages were defined. By the way, temperature variation can be monitored easily at the desired location of the flows, as demonstrated in Figure 1b.

The comprehensive list of parametric dimensions and the relations between the parameters for simulating the recuperator are given in Table 1. The pipe material was selected as steel with 0.08% Carbon content.

Table 1. Parameters and the relations in Simcenter Flomaster simulations.

Property	Value	Relations and constants intervals
Tube Arrangement	Aligned	-
No. of tube rows per pass	[TRP]	20-40
No. of tubes per row	[TR]	20-40
Tube transverse pitch [m]	[PT]	[Do]*1.5
Tube longitudinal pitch [m]	[PL]	[Do]*1.5
Tube material	Steel-Low Carbon 0.008%	Steel-Low Carbon 0.008%
Tube inner diameter [m]	[Di]	0.0127-0.03
Tube outer diameter [m]	[Do]	[Di]+0.0015
Tube length [m]	[TL]	2-3
Shell width [m]	[SW]	([TRP]+1)x[PL]
Shell length [m]	[SL]	2-3
Shell height [m]	[SH]	([TR]+1)x[PT]

According to the options given in Table 1, simulations were carried out for 135 different recuperator sizing in total.

1.3. Thermodynamic analysis

1.3.1. External Flow

In this study the tube arrangement over the banks of tubes were selected aligned arrangement. Diagonal pitch is calculated using the following equation;

$$S_D = \left[S_L^2 + \left(\frac{S_T}{2} \right)^2 \right] \tag{1}$$

For the aforementioned correlation, the Reynolds number $Re_{D,max}$ is based on the highest fluid velocity happening inside the tube bank,

$$Re_{D,max} = \frac{\rho V_{max} D}{\mu} \tag{2}$$

From the mass conservation requirement for an incompressible fluid, V_{max} occurs for the aligned arrangement at the transverse plane A_1 ,

$$V_{max} = \frac{S_T}{S_T - D} V \tag{3}$$

The pressure drop, which may be stated as, is directly related to the power needed to transport the fluid over the bank, which is frequently a significant operational expenditure,

$$\Delta P = N_L \chi \left(\frac{\rho V_{max}}{2} \right) f \tag{4}$$

Note that $\chi = 1$ for both square and equilateral triangle arrangements. Friction factor is obtained from the related diagrams from [reference] according to the Reynolds number.

Nusselt Number for external flow;

$$Nu = C Re^m Pr^{0.36} \left(\frac{Pr}{Pr_s} \right)^{0.25} \tag{5}$$

Here C and m are constants received from the related tables from reff [19] Pr and Prs are the Prandtl number under initial and average temperature values respectively.

The power required considering pressure drop;

$$\dot{W}_{pump} = \frac{\dot{m} \Delta P}{\rho} \tag{6}$$

1.3.2. Internal Flow

Due to the accuracy between $0.5 < Pr < 2000$ and $3 \times 10^3 < Re < 5 \times 10^6$ Gnielinski equation Nusselt number was calculated using the following;

$$\dot{m} = \rho u_m A_c \tag{7}$$

Re_D was calculated with Equation 8.

$$Re_D = \frac{4\dot{m}}{\pi D \mu} \tag{8}$$

The friction factor (f) in internal flow is a function of internal surface condition. It is unimportant on smooth surfaces but increases with the increase of internal surface roughness. Equation 6 was used due to giving best results on smooth surface conditions.

$$f = 0.316 Re_D^{-0.25}, Re_D \leq 2.10^4 \tag{9}$$

Nusselts number in internal flow was calculated with Equation 10.

$$Nu = \frac{\frac{f}{8}(Re-1000)Pr}{1+12.7(\frac{f}{8})^{0.5}(\frac{2}{Pr^3}-1)} \tag{10}$$

Heat convection coefficients for both flows are calculated using the following equation;

$$Nu = \frac{hL}{k} \tag{11}$$

Overall heat transfer coefficient U was calculated for the cylindrical shapes as given in Equation 12.

$$U = \frac{1}{\frac{1}{h_1} + \frac{r_1}{k} \ln \frac{r_2}{r_1} + \frac{r_1}{r_2} \frac{1}{h_2}} \tag{12}$$

1.4. Thermo-economic analysis

For economic savings to be maximum, the efficiency, the number of transfer units (NTU) and heat transfer surface area must be optimum. Therefore, the total saving S (\$/year) in a facility using thermal energy is given by Eq. 13 [20].

$$S = P - E \tag{13}$$

P (\$/year) is the annual profit gained by the recuperator's establishment as calculated in Eq. 2, and E (\$/year) is the yearly cost of the recuperator as calculated in Eq.'s 14-18.

$$P = (\kappa_h + \kappa_c) T_B \varepsilon C_{min} (T_{h,i} - T_{c,i}) \tag{14}$$

Where κ_h and κ_c are the thermal energy production unit cost and cooling unit cost of flue gas (\$/kWh), T_B is annual operating time, ε is the effectiveness of the heat exchanger, C_{min} is the minimum heat capacity.

$$E = \kappa_a A_{RZ} + (\dot{W}_h - \dot{W}_c) T_B \kappa_e \tag{15}$$

Where κ_a (\$/m²) is the unit cost of heat transfer surface area, κ_e electricity cost (\$/kWh), A_R (m²) is the overall

heat transfer surface area, and z (1/year) is the depreciation coefficient, \dot{W}_h (kW) power requirement for hot flow, \dot{W}_c (kW) power requirement for cold flow. The recuperator investment cost is defined as functions of thermal or size-related parameters to form the investment cost and the maintenance costs, interest rates and life of the plant as in Eq 16 [21]. The life of the recuperator is taken as five years, while the overall plant life is assumed as 30 years. Therefore, the investment cost of the recuperator is multiplied by six for a more precise product cost estimation. The thermal energy production unit cost required for the processes is calculated as 0.023 \$/kWh.

$$\dot{Z} = \frac{CRF \phi}{\tau} PEC_{Rec} \tag{16}$$

Where CRF is the capital recovery factor, ϕ is the maintenance factor. PEC is the purchase equipment cost of the recuperator, τ is the indicates the operating duration in seconds. CRF is defined as a function of interest rate (i) and annual operation period (n) as in Eq. (17)[22]:

$$CRF = \frac{i(1+i)^n}{(1+i)^n - 1} \tag{17}$$

Where the annual operation period, the maintenance factor, and the interest rate are taken to be as 8640 h, 1.12 and 15 %, respectively [23], PEC for the recuperator is calculated by Eq. (18) [24,25].

$$PEC_{Rec} = 2681 A_R^{0.59} \tag{18}$$

III. RESULTS AND DISCUSSIONS

In this study, the dimensions of a recuperator are optimized considering the economic gains. First, information such as flue gas mass flow rate, content, and operating conditions temperature were obtained. Then, flue gas temperature and its components have been defined in Simcenter Flomaster software together with component ratios to consider the changing thermophysical properties of the flue gas depending on the temperature. As a result of the simulations, heat exchanger areas, hot flow and cold flow outlet temperatures, total heat recovery, pressure drops for hot and cold flow and heat exchanger effectiveness were obtained for 135 different recuperator options. While . On the contrary, as the simulation number increases, savings values first increase and then decrease. For example, although maximum profit is observed in the 123rd simulation with 861 862 \$/year and minimum expense is observed in 7th simulation with 128 119 \$/year, Fig. 2 indicates 108th simulation that gives the

determining the optimum recuperator dimensions, the cost of the heat exchanger and the decrease in the fuel consumption occurring after heat recovery were considered. Therefore, recuperator sizes that maximize the annual savings were preferred, and results were discussed. As the simulation number increases in a general view of Fig. 2, the cost value increases as the recuperator dimensions increase.

Similarly, as the heat transfer surface area rises depending on the size of the heat exchanger, it increases the heat recovery, and the profit values also increase

maximum saving with 653 372 \$/year. Due to the maximum saving value, the optimum expense for the investment and maintenance of the recuperator and optimum profit after recuperator investment are observed as 189 358 \$/year and 842 730 \$/year, respectively.

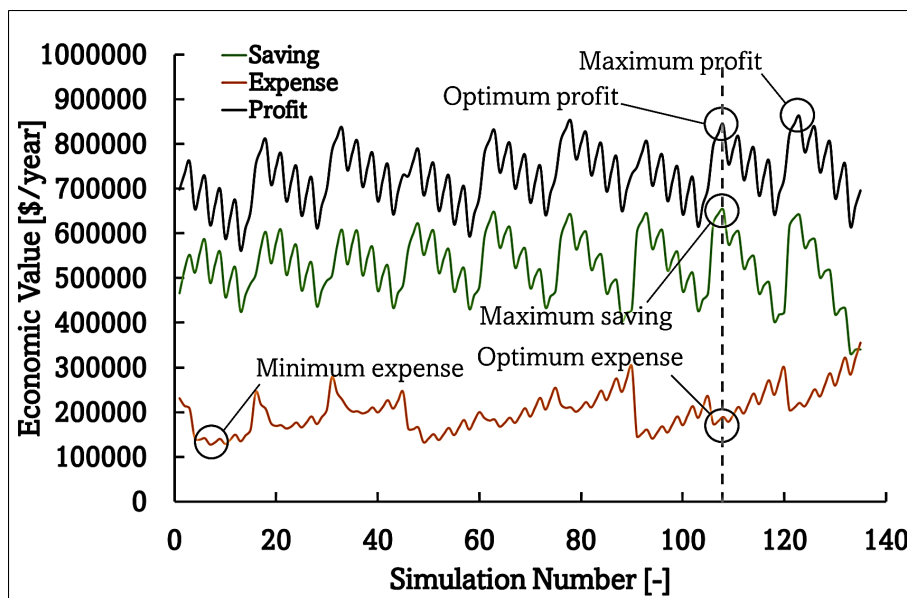


Figure 3. Economic evaluation versus simulation number.

When Fig. 3 is examined, it is seen that the highest cold flow outlet temperature and the lowest hot flow outlet temperature are in the 123rd simulation with 556.5 °C and 307.2 °C, respectively. The heat transfer surface area required to achieve these outlet temperatures is 428.2 m². Similarly, starting from Fig. 2, in the 108th simulation, which gives the highest economic saving value, the cold and hot flow outlet temperatures and heat transfer surface areas are 545.12 °C, 315.12 °C and

321.2 m², respectively. The heat transfer surface area determined in simulation 108 is exactly 25% lower than the 123rd simulation result, which gives the highest cold flow temperature and the lowest hot flow temperature. Whereas the cold flow outlet is 11.38 °C lower and the hot flow temperature is 7.92 °C higher. Therefore, with the minor losses in the outlet temperatures, the heat transfer surface area and investment cost are reduced significantly.

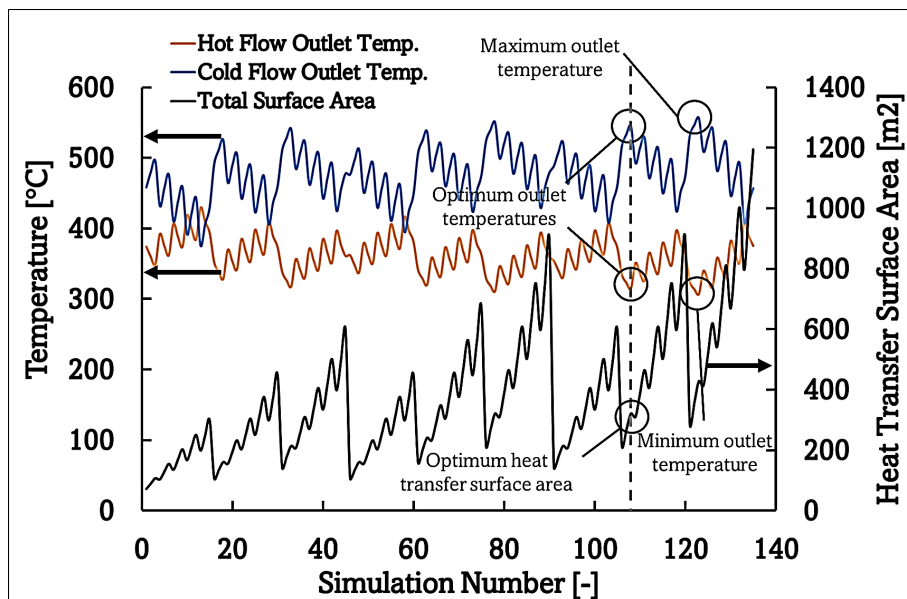


Figure 4. Outlet temperatures of flows and heat transfer surface area versus simulation numbers.

Fig. 4 shows the change in recuperator efficiency and heat recovery values. As a result of the 123rd simulation, where heat recovery and efficiency are the highest, efficiency and heat recovery are observed as 0.67 and 4660.7 kW, respectively. However, for the maximum

saving value, the optimum effectiveness and optimum heat recovery value were obtained as 0.65 and 4557.27 kW, respectively. Thus, 12 134 \$ higher annual saving is possible, with a minor decrease in heat recovery and efficiency.

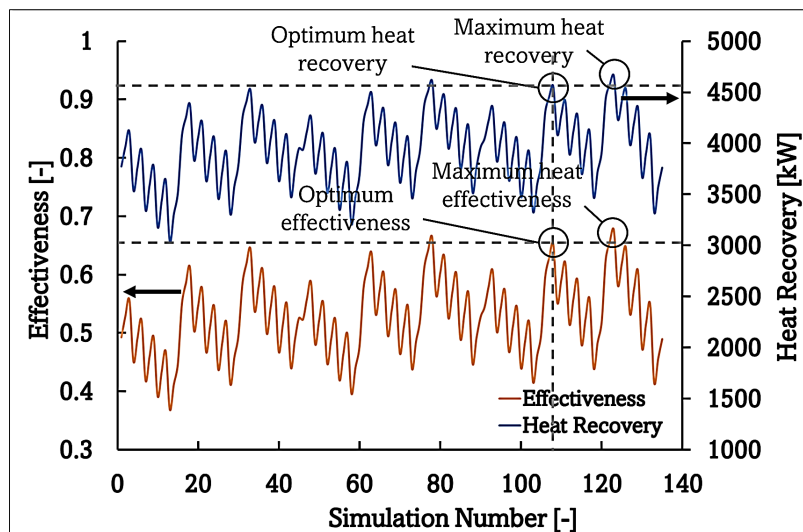


Figure 5. Effectiveness variation versus simulation numbers.

Figure 5 shows the pressure drops in hot and cold flow according to the simulation number. The highest-pressure drop is observed in both flows as 0.202 bar, in the 31st simulation in hot flow and the third simulation in cold flow. Since these pressure drops increase electricity consumption, the recuperator's annual

operating costs increase. In the 108th simulation, the optimum pressure drop for hot and cold flow is observed at 0.0225 bar and 0.0248 bar, respectively. The corresponding required power inputs for overcoming the pressure drops were given in Figure 6.

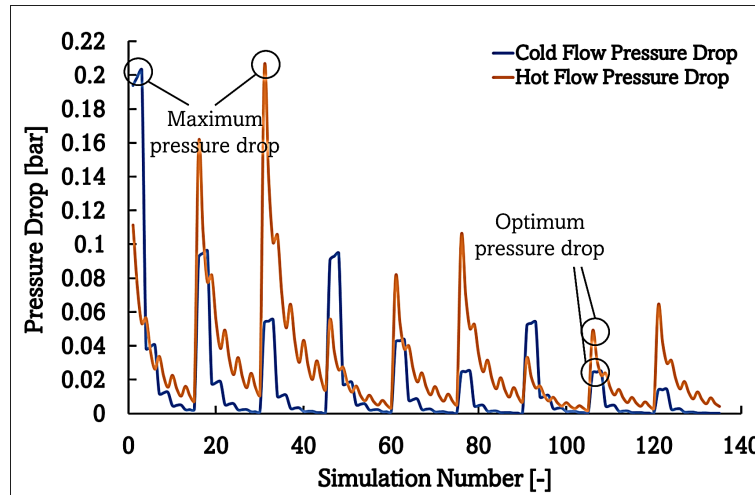


Figure 6. Pressure drop variation for hot side and cold side versus simulation number.

Pressure drops in heat exchangers in applications operating continuously for whole years cause electricity consumption tremendously depending on the volumetric flow rates and the constructions. Here, electricity consumption varies in a wide range between 1814.9 \$/year and 178654.2 \$/year due to pressure drops. For optimum pressure drop values, electricity

consumption for hot and cold flow is observed at 17409.80 \$/year and 10015.08 \$/year. The total electricity consumption for each flow is observed at 27424.89 \$/year. To understand the relation between the pressure drop and geometry of the recuperator, Figure 7 exhibits significant results.

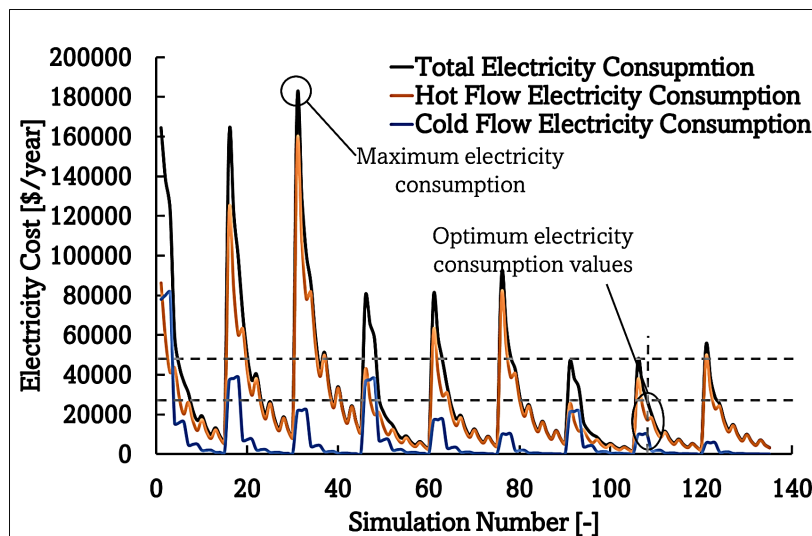


Figure 7. Electricity consumption for the pressure drops.

Figure 7a represents the geometric values of shell height (SH) and shell width (SW). SH and SW values increase depending on the number of tubes per row, number of tubes per row (TP), and tube rows per pass (TRP). Figure 7b demonstrates the repeating geometric values D_o , D_i , PL, and PT through the simulation, such

as the inner and outer diameter of the tubes and transverse and longitudinal pitches. According to the variations in geometric values in Figures 7a and 7b, the overall heat transfer coefficient (OHTC) variation is depicted in Figure 7c. According to the optimum values in simulation 108, OHTC is 107.04 W/m²K.

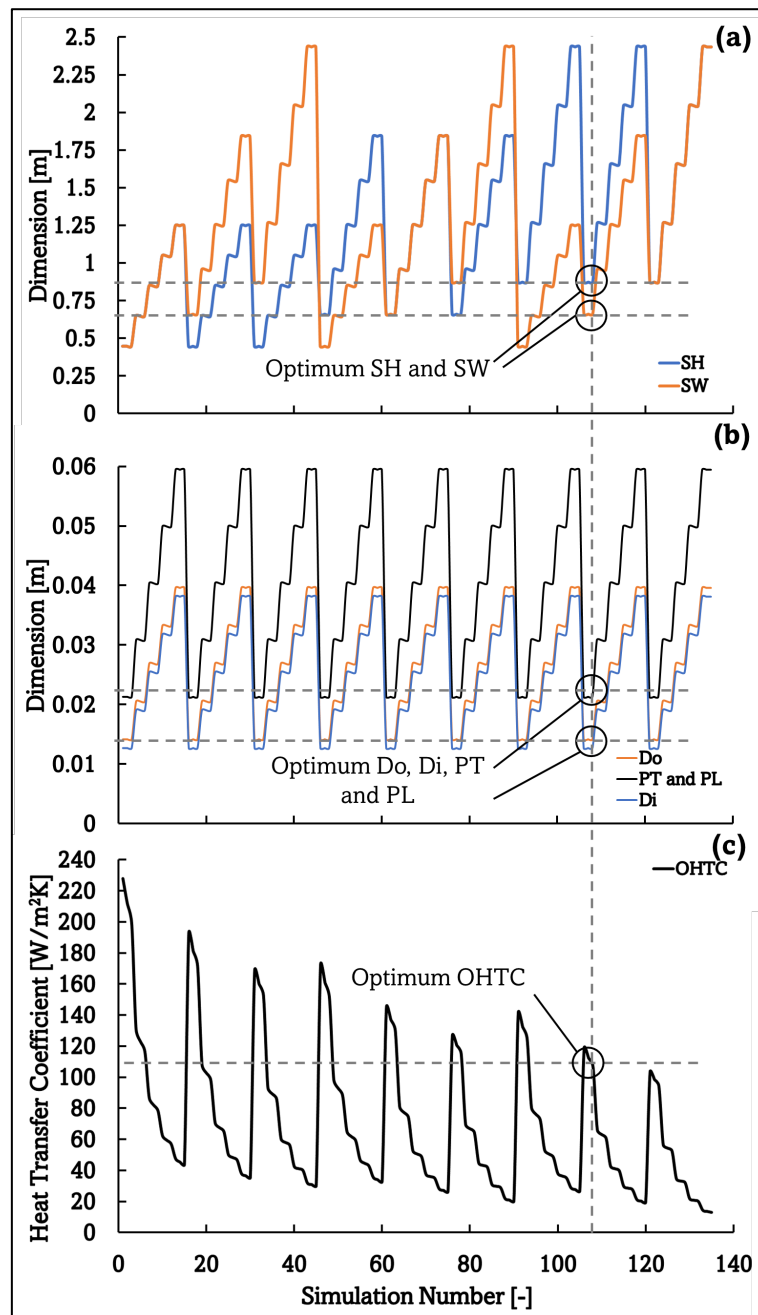


Figure 8. Overall heat transfer coefficient and recuperator dimensions versus simulation number.

The geometric and thermal results summarized in Figure 6 and Figure 7 are listed in Table 2 in detail for maximum saving. According to geometric properties in simulation 108, the Shell length and tube length are 3 m, inlet and outlet diameters of the tubes are 0.0127 m and 0.0142 m, respectively. The effectiveness of the recuperator is determined as 0.652, and outlet temperatures of the flow rates are observed as 315.12 °C and 545.11°C for hot and cold flow,

respectively. In addition, the Temperature distribution is monitored in detail in Figure 8 in the passages. Temperatures between hot and cold flow passages are 521.5 °C and 345.7 °C, respectively. Hence, the temperature increase of cold flow in the first passage is 325.7 °C, and in the second passage, 199.2 °C. In addition, the temperature decrease of hot flow in the first passage is 128.5 °C, and in the second passage, 206.38 °C.

Table 2. Optimum dimensions and properties in simulation 108.

Dimension	Value	Unit
[SL]	3	[m]
[Di]	0.0127	[m]
[Do]	0.0142	[m]
[TL]	3	[m]
[SW]	0.6603	[m]
[PT]	0.0213	[m]
[PL]	0.0213	[m]
[SH]	0.8733	[m]
Property		
OHTC	107.0396	[W/m ² K]
Hot Flow Outlet Temp.	315.1243	[°C]
Cold Flow Outlet Temp.	545.1196	[°C]
Total Surface Area	321.1964	[m ²]
Effectiveness	0.65247	[-]
Total Heat Recovery	4557.27	[kW]
Cold Flow Pressure Drop	0.024848	[bar]
Hot Flow Pressure Drop	0.022489	[bar]

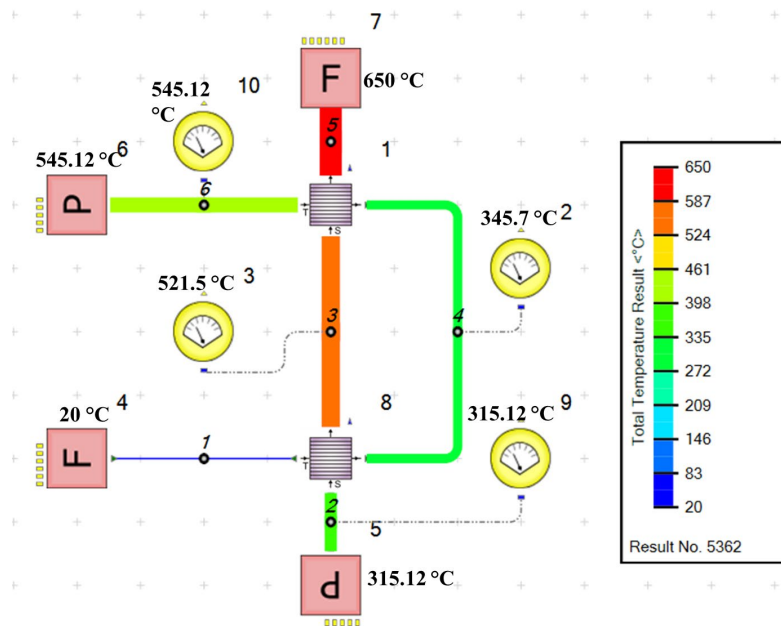


Figure 9. Temperature results for optimum parameters.

Considering the tubular recuperator optimization, the results obtained in this study seem to be compatible with the literature when compared with the results in the comprehensive review studies by [26] and [27].

IV. CONCLUSIONS

The gas-to-gas heat exchanger (recuperator) dimensions intended for an iron and steel plant have been optimized by considering economic parameters. Simulations were made for 135 different sizes in the recuperator by parameterizing the shell length, height, tube length, and longitudinal and transverse distances. For the recuperator's simulation results, the recuperator's investment costs and the energy consumption corresponding to the pressure drops were

calculated, and the optimum geometry that gives maximum savings was determined. As a result, the 108th simulation provided maximum savings with 653 252 \$ / year by using 321.19 m² of heat transfer surface area. As a future plan, the effects of a recuperator's behavior in dynamic operating conditions on furnace and chimney operating conditions and operating costs can be examined.

Nomenclature

Symbols

Ac: Crosssectional area [m²]
 H: heat convection coefficient [W/m²K]
 SD: Diagonal pitch [mm]
 SL: Longitudinal pitch [mm]
 ST: Transverse pitch [mm]
 V: velocity [m/s]
 D: diameter [mm]
 ρ: density [kg/m³]
 μ: dynamic viscosity [kg/ms]
 ΔP: pressure drop [bar]
 N: pipe number [-]
 γ: correction factor [-]
 f: friction factor [-]
 ε: Effectiveness [-]
 ṁ: massflow rate [kg/s]
 um: meal velocity [m/s]
 U: overall heat transfer coefficient [W/m²K]
 k: heat conductivity [W/mK]
 r: radius [mm]
 S: saving [\$ / year]
 P: profit [\$ / year]
 E: expense [\$ / year]
 α: unit cost [\$ / kWh]
 TB: Operating time [hour/year]

τ : operating duration [s]
 Z :cost rate [\$ / s]
 W :work [kW]
 z: depreciation coefficient [-]
 C: heat capacity [kW/K]
 T: temperature [°C]

Subscripts

L: longitudinal
 h: hot
 c: cold
 i: inlet
 o: outlet
 e: electrical
 R: recovery

Abbreviations

Nu: Nusselt number [-]
 PEC: purchase equipment cost [\$]
 Re: Reynolds number [-]
 Pr: Prandtl number [-]
 Rec: Recuperator
 CRF: capital recovery factor

ACKNOWLEDGMENT

We thank Karabuk University for providing its software and hardware infrastructure to realize the current study.

Conflict of Interest

The authors declare that they have no conflict of interest

REFERENCES

- [1] Pashchenko D, Nikitin M. Forging furnace with thermochemical waste-heat recuperation by natural gas reforming: Fuel saving and heat balance. *Int J Hydrogen Energy* 2021;46:100–9. <https://doi.org/10.1016/j.ijhydene.2020.09.228>.
- [2] Pashchenko D. How to choose endothermic process for thermochemical waste-heat recuperation? *Int J Hydrogen Energy* 2020;45:18772–81. <https://doi.org/10.1016/j.ijhydene.2020.04.279>.
- [3] Wang RQ, Jiang L, Wang YD, Roskilly AP. Energy saving technologies and mass-thermal network optimization for decarbonized iron

- and steel industry: A review. *J Clean Prod* 2020;274:122997.
<https://doi.org/10.1016/j.jclepro.2020.122997>.
- [4] Kayabasi E, Kurt H. Simulation of heat exchangers and heat exchanger networks with an economic aspect. *Eng Sci Technol an Int J* 2018;21:70–6.
<https://doi.org/10.1016/j.jestch.2018.02.006>.
- [5] Tom B, Kayabasi E. Design and simulation of a microchannel heat exchanger for cooling a micro processor using ethylene. *El-Cezeri J Sci Eng* 2021;8:1243–53.
<https://doi.org/10.31202/ecjse.909855>.
- [6] Seong BG, Hwang SY, Kim KY. High-temperature corrosion of recuperators used in steel mills. *Surf Coatings Technol* 2000;126:256–65.
[https://doi.org/10.1016/S0257-8972\(00\)00523-5](https://doi.org/10.1016/S0257-8972(00)00523-5).
- [7] Dawood TA, Raphael R, Barwari I, Akroot A. Solar Energy and Factors Affecting the Efficiency and Performance of Panels in Erbil / Kurdistan Solar Energy and Factors Affecting the Efficiency and Performance of Panels in Erbil / Kurdistan. *Int J Heat Technol* 2023;41:304–12.
<https://doi.org/10.18280/ijht.410203>.
- [8] Bdaiwi M, Akroot A, Abdul Wahhab HA, Assaf YH, Nawaf MY, Talal W. Enhancement Heat exchanger performance by insert dimple surface ball inside tubes: A review. *Results Eng* 2023;19:101323.
<https://doi.org/10.1016/J.RINENG.2023.101323>.
- [9] Kareem AF, Akroot A, Wahhab HAA, Talal W, Ghazal RM, Alfaris A. Exergo – Economic and Parametric Analysis of Waste Heat Recovery from Taji Gas Turbines Power Plant Using Rankine Cycle and Organic Rankine Cycle. *Sustainability* 2023;15:9376.
- [10] Shafiey Dehaj M, Hajabdollahi H. Fin and tube heat exchanger: Constructal thermoeconomic optimization. *Int J Heat Mass Transf* 2021;173:121257.
<https://doi.org/10.1016/j.ijheatmasstransfer.2021.121257>.
- [11] Söylemez MS. On the thermoeconomical optimization of heat pipe heat exchanger HPHE for waste heat recovery. *Energy Convers Manag* 2003;44:2509–17.
[https://doi.org/10.1016/S0196-8904\(03\)00007-4](https://doi.org/10.1016/S0196-8904(03)00007-4).
- [12] Manjunath K, Sharma OP, Kaushik SC. Entropy generation and thermoeconomic analysis of printed circuit heat exchanger using different materials for supercritical CO₂ based waste heat recovery. *Mater Today Proc* 2020;21:1525–32.
<https://doi.org/10.1016/j.matpr.2019.11.077>.
- [13] Sahin B, Ust Y, Teke I, Erdem HH. Performance analysis and optimization of heat exchangers: a new thermoeconomic approach. *Appl Therm Eng* 2010;30:104–9.
<https://doi.org/10.1016/j.applthermaleng.2009.07.004>.
- [14] Maghsoudi P, Sadeghi S, Khanjarpanah H, Gorgani HH. A comprehensive thermoeconomic analysis, optimization and ranking of different microturbine plate-fin recuperators designs employing similar and dissimilar fins on hot and cold sides with NSGA-II algorithm and DEA model. *Appl Therm Eng* 2018;130:1090–104.
<https://doi.org/10.1016/j.applthermaleng.2017.11.087>.
- [15] Liu Z, Cheng H. Multi-objective optimization design analysis of primary surface recuperator for microturbines. *Appl Therm Eng* 2008;28:601–10.
<https://doi.org/10.1016/j.applthermaleng.2007.04.010>.
- [16] Hu H, Guo C, Cai H, Jiang Y, Liang S, Guo Y. Dynamic characteristics of the recuperator thermal performance in a S–CO₂ Brayton cycle. *Energy* 2021;214:119017.
<https://doi.org/10.1016/j.energy.2020.119017>.
- [17] Chen H, Liu Y wen. A new optimization concept of the recuperator based on Hampson-type miniature cryocoolers. *Energy* 2021;224:120091.
<https://doi.org/10.1016/j.energy.2021.120091>.
- [18] Siemens. Simcenter Flomaster™ User Guide. 2020.
- [19] Cengel YA. *Heat Transfer: A Practical Approach*. 2nd ed. McGraw-Hill; 2003.
- [20] Kardos J, Strelow O, Walde R. Bewertung und Optimierung des Wärmerückgewinns in Rekuperatorsystemen. *Chem Tech* 1983;35:71–4.
- [21] Yuksel YE, Ozturk M. Thermodynamic and thermoeconomic analyses of a geothermal energy based integrated system for hydrogen production. *Int J Hydrogen Energy* 2017;42:2530–46.
<https://doi.org/10.1016/j.ijhydene.2016.04.172>.
- [22] Tozlu A, Kayabasi E, Ozcan H. Thermoeconomic analysis of a low-temperature waste-energy assisted power and hydrogen plant at off-NG grid region. *Sustain Energy Technol Assessments* 2022;52:102104.
<https://doi.org/10.1016/j.seta.2022.102104>.
- [23] Tozlu A, Abuşoğlu A, Özahi E. Thermoeconomic analysis and optimization of a Re-compression supercritical CO₂ cycle using waste heat of Gaziantep Municipal Solid Waste Power Plant. *Energy* 2018;143:168–80.
<https://doi.org/https://doi.org/10.1016/j.energy.2017.10.120>.
- [24] Zhang Q, Ogren RM, Kong SC. Thermo-

- economic analysis and multi-objective optimization of a novel waste heat recovery system with a transcritical CO₂ cycle for offshore gas turbine application. *Energy Convers Manag* 2018;172:212–27. <https://doi.org/10.1016/j.enconman.2018.07.019>.
- [25] Ozcan H, Kayabasi E. Thermodynamic and economic analysis of a synthetic fuel production plant via CO₂ hydrogenation using waste heat from an iron-steel facility. *Energy Convers Manag* 2021;236:114074. <https://doi.org/10.1016/j.enconman.2021.114074>.
- [26] Xiao G, Yang T, Liu H, Ni D, Ferrari ML, Li M, et al. Recuperators for micro gas turbines: A review. *Appl Energy* 2017;197:83–99. <https://doi.org/10.1016/j.apenergy.2017.03.095>.
- [27] Reznicek EP, Neises T, Braun RJ. Optimization and techno-economic comparison of regenerators and recuperators in sCO₂ recompression Brayton cycles for concentrating solar power applications. *Sol Energy* 2022;238:327–40. <https://doi.org/10.1016/j.solener.2022.03.043>.